# An Energy Efficient Power Controller Switching Methodology for an Ambient Healthcare Network.

Michael Walsh, Brendan O'Flynn, John Barton and Cian O'Mathuna
Clarity Centre for Sensor Web Technologies
Tyndall National Institute
University College Cork, Cork, Ireland
Email: www.michael.walsh@tyndall.ie

***Abstract*—A methodology for improved power controller switching in mobile Body Area Networks operating within the ambient healthcare environment is proposed. The work extends Anti-windup and Bumpless transfer results to provide a solution to the ambulatory networking problem that ensures sufficient biometric data can always be regenerated at the base station. The solution thereby guarantees satisfactory quality of service for healthcare providers. Compensation is provided for the nonlinear hardware constraints that are a typical feature of the type of network under consideration and graceful performance degradation in the face of hardware output power saturation is demonstrated, thus conserving network energy in an optimal fashion.**

## I. Introduction

Ubiquitous or pervasive Body Area Networks (BANs) and their use in the healthcare application space are now beginning to reach a level of maturity wherein a number of innovative solutions are at advanced stages of commercial development. To maximise BAN market penetration these systems should be robust, power aware, mobile, low cost and be readily implementable in a healthcare environment. This paper illustrates how recent developments in the area of systems science can help in this endeavor. In particular it is shown how Anti-Windup(AW) and Bumpless Transfer (BT) power control techniques can be applied to the design of next generation BANs that can address the aforementioned issues in an intuitively appealing manner.

Although the processing of relevant biometric information can consume valuable energy, it is clear that data transmission is the primary constraint on battery life in a BAN and can account for 70-90% of power usage [1]. The benefits of transmission power control are obvious when there exists a need for the BAN to remain operational for extended periods of time and to this end a number of wireless network power control algorithms have already been proposed [2], [3]. These schemes have exhibited some success in extending battery lifetime while concurrently providing pre-specified levels of quality of service (QoS). This equates to the provision of sufficient data to reassemble biometric waveforms, (e.g. ECG, EEG, blood oxygen levels, pulse ect.), or to reliably detecting the movement of an elderly person, in an ambient fashion, be they at home or in a care facility.

## II. Performance Constraints in a typical Body Area Network

A variety of limits on performance surface sooner rather than later in any practical BAN. This section outlines the constraints that are treated by this work.

### A. Hardware Limitations

When employing embedded systems in miniaturised BAN applications a number of hardware related factors are an inevitable constraint on performance. For instance the limited, necessarily quantised, and quite often saturated transceiver output power of a typical mobile node can severely degrade network performance, ultimately leading to instability if not properly addressed. This paper provides a novel example of how to address these types of unavoidable nonlinear constraints in an optimal fashion.

### B. Network Coverage

Another major challenge lies in maximizing network coverage area. Given that many of the "off-the-shelf" sensor node platforms operate using low power 802.15.4 type wireless technologies, transmission range is extremely limited, especially in the indoor environment. A multihop or mesh network topology is often proposed to extend coverage area necessitating the introduction of a power controller switching protocol. Fig. 1(a) illustrates the type of scenario that is envisaged whereby subject X is being monitored and is wearing (perhaps a number of) wireless biometric devices. Initially X is in communication with base station $BS_1$. When X moves to an adjoining area in an ambulatory fashion, data must at some point be transmitted via $BS_2$ rather than $BS_1$ quite possibly within a mesh paradigm. It is crucial that the QoS and energy efficient properties of the BAN be retained in such a scenario. Here BT, [4], is employed to optimise this process. In the proposed BT scheme a global controller oversees multiple local loop controllers that are designed to ensure that the mesh is power aware. Depending on certain performance requirements, a sequence of switches are necessary between each controller. In essence, one controller will be operational or "on-line" while the other candidate controller(s) must be deemed "off-line" at any instant. Clearly it is necessary to be able to switch between these controllers (located at adjacent base stations) in a stable fashion. This paper presents sufficient

978-1-4244-4641-4/09/$25.00 ©2009 IEEE

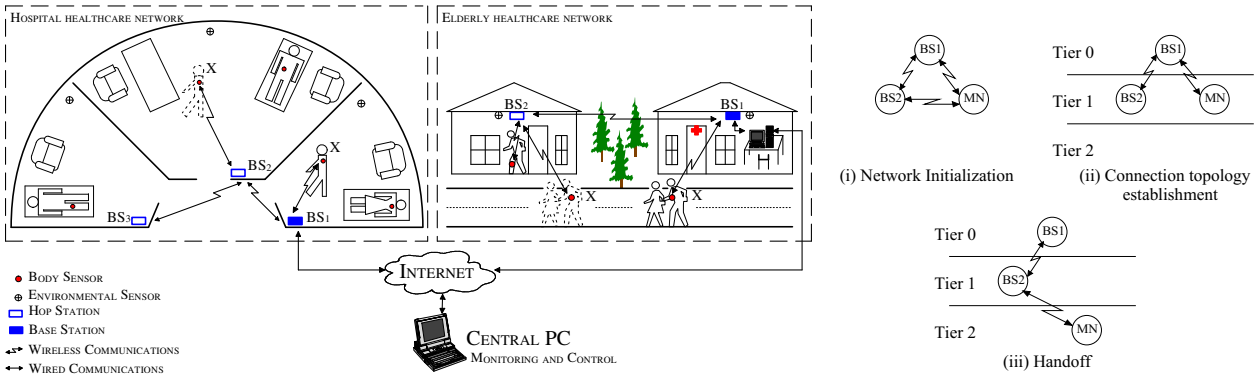


Fig. 1. (a) The ambient healthcare environment. Power control for X is initially handled by $BS_1$. Subject X then moves in an ambulatory fashion and data is now multihopped via $BS_2$ to $BS_1$ and $BS_2$ handles power control for X. Hence power controller switching has occurred between $BS_1$ and $BS_2$, (b) Simple WSN multihop power controller switching scenario.

conditions to ensure that the induced transient signals are bounded, thereby satisfying network stability requirements. To achieve this smoothly, the gap between the off and online control signals must be bounded so that the control signal driving the plant cannot induce instability. In this work both AW and BT are applied in tandem for the first time in a wireless network, thereby providing effective control of the signal entering the 'plant' (in this case the node transceiver) at any instant For the remainder of the work the term anti-windup-bumpless-transfer or AWBT is coined to denote the new technique.

## III. Formal Statement of The Switching Problem: Two Base Station Scenario

To determine when power controller switching should occur the filtered downlink received signal strength indicator (RSSI) signal or the RSSI signal is considered at the mobile node. It is assumed that each base station or access point will possess the ability to transmit at a predefined maximum power level within some quantisation structure at any instant. Initially, the two node mobile ad-hoc WSN scenario depicted in Fig. 1(b)(i) is considered. When the network initializes it is assumed that the Mobile Node (MN) is unaware of its position and is transmitting data using maximum transmission power to all "listening" base stations.

The MN will subsequently receive data packets from each base station within range (in this scenario limited to BS1 and BS2). A downlink RSSI is now calculated for each received packet. The signals are compared with a predefined threshold value. This threshold ensures that the base station is located in the highest possible tier of the BAN hierarchy and is also within range of the mobile node that will have routing precedence, thereby satisfying a minimal latency requirement within the network.

From Fig. 1(b)(ii) and following network initialization, MN is now located in tier 1 of the mesh hierarchy and BS1, located in tier 0, dynamically manages the MN's power based on the uplink RSSI observed at BS1. At some future sampling instant, due to mobility MN joins tier 2 in the hierarchy, see Fig. 1(b)(iii) and power control for MN is now implemented through the uplink RSSI at BS2.

## IV. Modelling The Network

The goal of this work is to dynamically adjust the mobile node transmitter power in a distributed manner, so that the power consumption is minimized while also maintaining sufficient transmission quality. A direct measurement of QoS is therefore an a priori requirement. In the past it has been suggested that uplink RSSI was a less than ideal metric for power control, however this claim was based on experimentation with early platforms using older radios. More recently developed 802.15.4 compliant radios such as the TI CC2420, have been shown to exhibit highly stable performance and it is now commonly held that for a given link, RSSI exhibits acceptably small time-variability [5]. In this work the received signal strength indicator (RSSI) is therefore selected as the feedback variable to manage the control objective.

In [1] a method was introduced to directly estimate the signal to noise plus interference ratio (SINR) using RSSI measurements. From [1] the SINR $\gamma(k)$, in terms of RSSI is given by

$$\gamma(k) \approx RSSI(k) - n(k) - C - 30 \qquad (1)$$

where the addition of the scalar term 30 accounts for the conversion from dBm to dB, $n(k)$ is thermal noise and C is the measurement offset assumed to be 45 dB.

A setpoint or reference RSSI value can therefore be selected and related directly to PER, as outlined in the 802.15.4 standard [6]. To expand, the bit error rate (BER) for the 802.15.4 standard operating at a frequency of 2.4GHz is given by

$$BER = \frac{8}{15} \times \frac{1}{16} \times \sum_{k=2}^{16} -1^k \begin{pmatrix} 16 \\ k \end{pmatrix} e^{20 \times SINR \times (\frac{1}{k} - 1)}, \qquad (2)$$

and given the average packet length for this standard is 22 bytes, the PER can be obtained from

$$PER = 1 - (1 - BER)^{PL} \tag{3}$$

where $PL$ is packet length including the header and payload. PER is more useful here given the transceiver used to validate the proposed methodology, is based on a wideband transceiver, transmitting and receiving data in packet rather then bit format. Establishing a relationship between RSSI, SINR, BER and subsequently PER can therefore help to pre-specify levels of system performance.

### A. The System Model

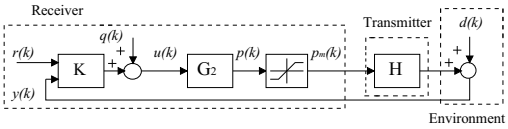


Fig. 2. Wireless System Model with saturation block at the output.

A systems science representation of a single base station communicating to a single mobile node is illustrated in Fig. 2. The system has reference input $r(k)$ (reference RSSI), the value for which is determined using (1), (2) and (3) above, guaranteeing a predefined PER. $q(k)$ is quantization noise introduced as a result of switching between discrete power levels. The controller $K(z)$ has controller output $u(k)$ and takes the form $K(z) = [K_1(z)\ K_2(z)]$ a standard two degree of freedom structure.

The plant $G(z)$ is represented by $G(z) = [G_1(z)\ G_2(z)]$, where $G_1(z)$ and $G_2(z)$ are the disturbance feedforward and feedback parts of $G(z)$ respectively. Given no structured disturbance model is available in the form of a transfer function, $G_1(z)$ is taken to be $G_1 = I$, where $I$ is the identity matrix. $G_2(z)$ is a low pass filter with sufficient bandwidth to eliminate quantization noise. $G_2(z)$ is selected as

$$G_2(z) = \frac{1}{1.1z - 0.9}. \tag{4}$$

$G_2(z)$ outputs a power level update $p(k)$, which in turn is transmitted to the mobile node. The mobile node transmitter has inherent upper and lower bounds on hardware transmission power output, represented in Fig. 2 by the saturation block, the output for which is saturated output power or $p_m(k)$. $H$ represents the hardware switch in the mobile node's transceiver and is taken here to be the identity matrix or $H = I$. $d(k)$ is a disturbance to the system and comprises of channel attenuation, interference and noise.

### B. Mapping the Saturation Function

For this scenario a problem presents itself in that the saturation constraint is located at the output of the system and while there have been some advances in control design theory to deal with this type of output constraint [7], there is a vast literature covering the treatment of linear systems subject to input saturation constraints, see [8] and references therein.

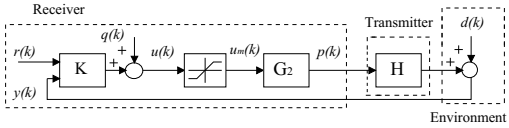


Fig. 3. Wireless System Model with saturation block mapped from the output to the input of the system.

A solution outlined in [2] and illustrated in figure 3 lies in the mapping of the output saturation constraint to the input of the plant or the output of the controller.

### C. The Power Controller Switching Problem

Figure 4 illustrates the power controller switching problem for a two base station, one mobile node scenario. $K_{BS1}$ and $K_{BS2}$ are the same construct as $K(z)$ from the previous section. Base station 1 is deemed "on-line" and is therefore controlling the mobile node's transmission power. The difficulty in switching between base station 1 and base station 2 is as a result of the possible difference between $p_1(k)$ and $p_2(k)$ at the time of switching. This discrepancy can exist due to incompatible initial conditions and can induce an unwanted transient and possible instability in the system. The result can be a disruption of vital health status data or indeed a loss in service altogether.

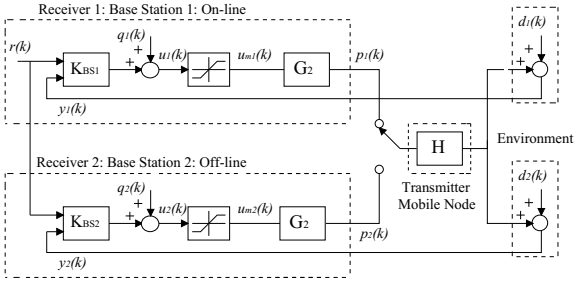


Fig. 4. Wireless System Model with power controller switching.

An additional difficulty arises that is unique to the wireless case. As mentioned previously, in order for AWBT to be effective, the feedback measurement observed at the "off-line" controller must be sufficiently close in magnitude to the feedback measurement observed at the "on-line" controller. Clearly from Fig. 4 $d_1(k) \neq d_2(k)$ due to differing propagation environments. This disparity can mean AWBT is unable to eliminate the difference between $u_{m1}(k)$ and $u_{m2}(k)$ therefore a more complex control design solution is required. However prior to solving this, a linear controller must be synthesized. This controller provides pre-specified levels of stability and performance in the nominal linear closed loop i.e. when neither saturation nor switching is occurring. Following this a conservative anti-windup design is used to address the hardware saturation constraint. Finally a modification is made to the AWBT scheme to account the differing feedback signals and to enable seamless power controller switching.

## V. ANTI-WINDUP DESIGN

The technique employed here implements a two step AWBT design procedure. The first step is to design a linear power controller ignoring the inherent nonlinear constraints on the system. The second step involves using recent advances in AW theory, to minimize degradation in the face of actuator constraints. The technique employed here is the Weston - Postlethwaite Anti-Windup Bumpless Transfer (WP-AWBT) synthesis technique. First presented in [9] and later in its discretized form in [10], this approach uses an $\mathcal{L}_2$ approach in conjunction with linear matrix inequality (LMI) optimization techniques to ensure that during saturation the systems performance remains as close to nominal linear operation as possible and returns to the linear operational region as quickly as possible.

### A. Robust Linear Power Tracking Controller Design

Quantitative feedback theory (QFT) provides an intuitively appealing means of guaranteeing both robust stability and performance and is essentially a Two-Degree-of-Freedom (2DOF) frequency domain technique, as illustrated in figure 4. In a QFT design, the responsibility of the feedback compensator, $K_2(z)$, is to focus primarily on attenuating the undesirable effects of uncertainty, disturbance and noise. Having arrived at an appropriate $K_2(z)$, a pre-filter $K_1(z)$, is then designed so as to shift the closed-loop response to the desired tracking region, again specified *a priori* by the engineer. The approach requires that the designer select a set of desired specifications in relation to the magnitude of the frequency response of the closed-loop system, thusly achieving robust stability *and* performance. The design procedure in its entirety is omitted here due to space constraints, however the interested reader is directed to [11] and references therein. Using this technique $K_2(z)$ was found to be

$$K_2(z) = \frac{z - 0.6622}{0.7103z - 0.7103} \tag{5}$$

guaranteeing a phase and gain margin equal to $50^\circ$ and $1.44$, respectively. The closed-loop transfer function is shaped using $K_1(z)$ ensuring the system achieves steady state around the target value of $5 \leq t_{ss} \leq 25(s)$ and a damping factor of $\xi = 0.5$ is selected to reduce outage probability at the outset of communication. The resultant $K_1(z)$ is

$$K_1(z) = \frac{1.4127z}{z - 0.4127} \tag{6}$$

### B. WP-AWBT Synthesis

Consider the generic AW configuration shown in figure 5(a). As illustrated above the plant takes the form $G = [G_1\ G_2]$, the linear controller is represented by $K = [K_1\ K_2]$ where

$$K(z) \sim \begin{cases} x_c(k+1) = A_c x_c(k) + B_c y_{lin}(k) + B_{cr} r(k) \\ u_{lin}(k) = C_c x_c(k) + D_c y_{lin}(k) + D_{cr} r(k) \end{cases} \tag{7}$$

$\Theta = [\theta_1\ \theta_2]$ is the AW controller becoming active only when saturation occurs. Given the difficulty in analyzing the stability and performance of this system we now adopt a framework

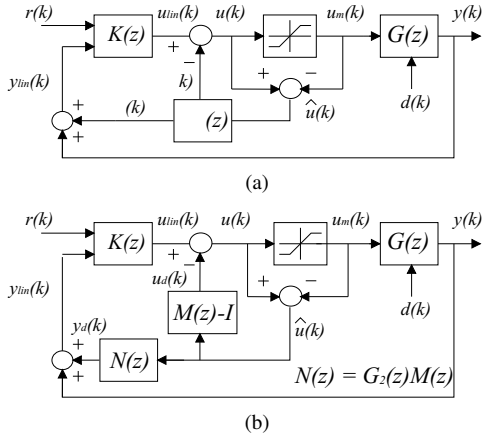


Fig. 5. (a) A generic anti-windup scenario, (b) Weston Postlethwaite Anti-Windup conditioning technique.

first introduced in [9] for the problem at hand. This approach reduces to a linear time invariant Anti-Windup scheme that is optimized in terms of one transfer function $M(z)$ shown in figure 5(b). It was shown in [9] that the performance degradation experienced by the system during saturation is directly related to the mapping $\mathcal{T} : u_{lin} \rightarrow y_d$. Note that from figure 5(b) $M - I$ is considered for stability of $\mathcal{T}$ and $G_2 M$ determines the systems recovery after saturation, where $I$ is the identity matrix. This decoupled representation visibly shows how this mapping can be utilized as a performance measure for the AW controller. To quantify this we say that an AW controller is selected such that the $\mathcal{L}_2$-gain, $\|\mathcal{T}\|_{i,2}$, of the operator $\mathcal{T}$

$$\|\mathcal{T}\|_{i,2} = \sup_{0 \neq u_{lin} \in \mathcal{L}_2} \frac{\|y_d\|_2}{\|u_{lin}\|_2}$$

where the $\mathcal{L}_2$ norm $\|x\|_2$ of a discrete signal $x(h), (h = 0, 1, 2, 3, ....)$ is

$$\|x\|_2 = \sqrt{\sum_{h=0}^{\infty} \|x(h)\|^2}$$

*1) Static anti-windup synthesis::* Static AW has an advantage in that it can be implemented at a much lower computational cost and adds no additional states to the closed loop system. As extra modes are undesirable it stands to reason that minimal realizations of the controller and plant should be used. The methodology for obtaining such realizations is outlined in [10]. LMI synthesis routine is subsequently employed considering the plant given by (4) and the linear controller (5) and the resultant controller $\Theta = [\Theta_1' \Theta_2'] = [-0.2049\ 0.6377]'$ is obtained using the LMI toolbox in Matlab[1].

## VI. MODIFIED AWBT DESIGN

### A. Motivation

To motivate the need for the proposed modification to the above AWBT technique, the reader is directed to Fig. 4. As

[1]The Mathworks Inc.

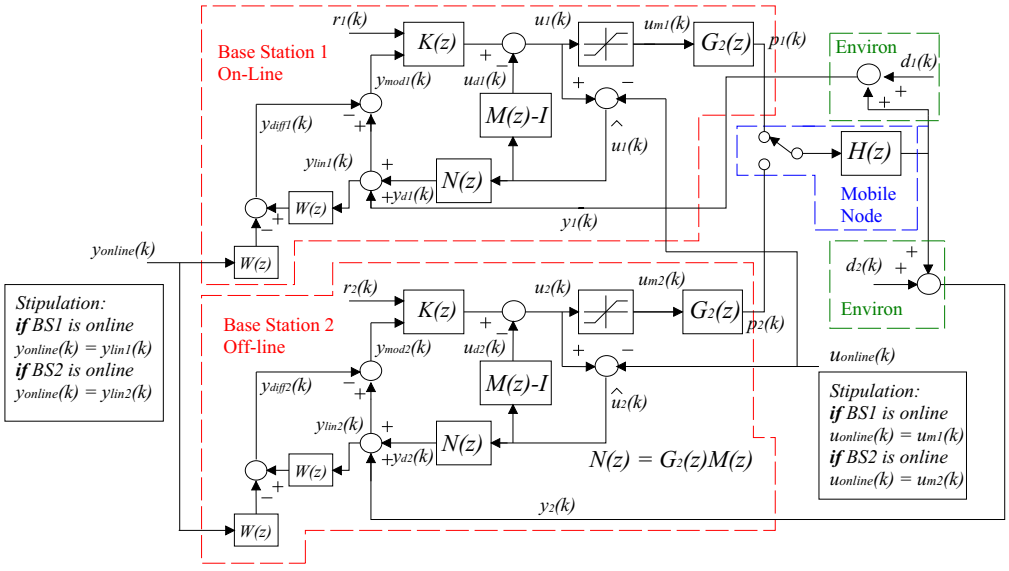


Fig. 6. The proposed modified WP-AW scheme, 2 Base Station Scenario.

mentioned previously traditional AWBT schemes require that the feedback signal entering the "off-line" controller equals or is close in magnitude to the feedback signal entering the "on-line" controller. Clearly from Fig. 4 this is not the case as $d_1(k) \neq d_2(k)$ due to differing propagation environments. As a result the AWBT controller in Fig. 5(b) cannot guarantee the controller outputs for both the "off-line" and "on-line" controllers are equal in magnitude. The result can be an unwanted transient at switching due to the incompatible controller values, possibly causing vital health status information to be lost or a total breakdown in communication.

### B. Proposed Solution

The following modification compensates for the inherent discrepancy in feedback RSSI signals between the "off-line" and the "on-line" controllers. Fig. 6 illustrates the modification to the system. Consider the "off-line" controller base station 2, where an additional signal $y_{diff2}(k)$ is included in the feedback signal. This signal comprises of

$$y_{diff2}(k) = -y_{online}(k)W(z) + y_{lin2}(k)W(z) \qquad (8)$$

where $W(z)$ is a low pass filter removing the high frequency component present in each of the feedback RSSI signals. Note that $y_{online}(k)$ is determined by which base station is online. Therefore $y_{online}(k) = y_{lin1}$ given $BS1$ is online. The signal driving the "off-line" controller then becomes

$$y_{mod2}(k) = y_{lin2}(k) - y_{diff2}(k) =$$
$$y_{lin2}(k) + y_{lin1}(k)W(z) - y_{lin2}(k)W(z)$$
$$y_{mod2}(k) = y_{lin1}(k)W(z) + y_{lin2}(k)(1 - W(z)) \qquad (9)$$

which comprises of the "dc" or low frequency component of the "on-line" feedback signal or $y_{lin1}(k)W(z)$ and the high frequency component of the "off-line" control signal $y_{lin2}(k)(1 - W(z))$. Each of these signals are incorporated in the design for different reasons. Firstly driving the "off-line controller" with the "dc" component of the "on-line" control signal will ensure both controller outputs will be approximately equal or $u_1(k) \approx u_2(k)$. Retaining the high frequency component of the "off-line" feedback signal enables the "off-line" controller with the ability to compensate for deep fades in it's own feedback signal. Should power controller switching then occur a large transient is avoided as the feedback conditions are compatible.

Should base station 2 become "on-line" equation (9) becomes

$$y_{mod2}(k) = y_{lin2}(k) - y_{diff2}(k) = y_{lin2}(k) +$$
$$y_{lin2}(k)W(z) - y_{lin2}(k)W(z) = y_{lin2}(k) \qquad (10)$$

hence the modification has no effect on the system and the AWBT scheme operates as normal. This approach in essence adds a filtered additional disturbance to the system which is intuitively appealing given a perturbation of the disturbance feedforward portion of the plant $G_1$ will have no bearing on stability [7].

## VII. SIMULATION AND DISCUSSION

This section analyses the system response firstly without AWBT, then with the introduction of AWBT and finally with the modified AWBT design in place.

### A. System Parameters and Performance Criteria

A sampling frequency of $T_s = 1(sec)$ is used throughout and a target RSSI value of $-55$dBm is selected for tracking, guaranteeing a PER of $< 1\%$, verified using equations (2), (3) and (1). The *standard deviation* of the RSSI tracking error is chosen as a performance criterion:

$$\sigma_e = \left\{ \frac{1}{S} \sum_{k=1}^{S} [r(k) - RSSI(k)]^2 \right\}^{\frac{1}{2}} \qquad (11)$$

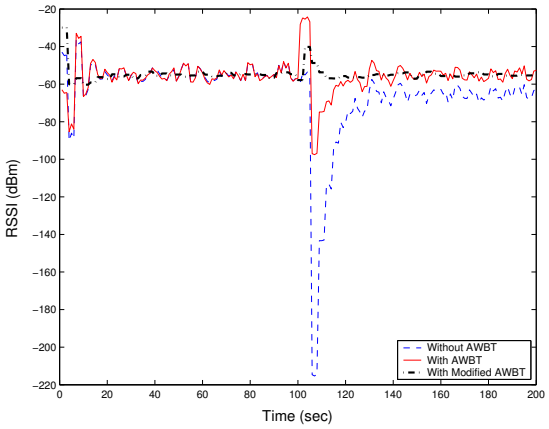


Fig. 7. Modified AWBT performance ignoring saturation constraints and where power controller switching occurs at 100 (sec)

TABLE I
SIMULATION RESULTS. CHARACTERISTICS: $\sigma_e$ - STANDARD DEVIATION (DBM), $P_o$ - OUTAGE PROBABILITY (%), $P_{av}$ - AVERAGE POWER CONSUMPTION (MW)

| | **Without AWBT** | **With AWBT** | **Modified AWBT** |
|---|---|---|---|
| $\sigma_e$ | 30.59 | 4.445 | 1.603 |
| $P_o$ | 63.77 | 31.88 | 8.696 |
| $P_{av}$ | 1 | 0.199 | 0.158 |

where $S$ is the total number of samples and $k$ is the index of these samples. *Outage probability* is defined as

$$P_o(\%) = \frac{number\ of\ times\ RSSI\ <\ RSSI_{th}}{the\ total\ number\ of\ iterations} \times 100 \quad (12)$$

where $RSSI_{th}$ is selected to be $-57$dBm, a value below which performance is deemed unacceptable in terms of PER. This can be easily verified again using equations (1), (2) and (3). To fully access each paradigm, some measure of power efficiency is also useful and here we define *average power consumption* in milliwatts as

$$P_{av} = 10^{\left[\left\{\frac{1}{S}\sum_{k=1}^{S} p_{dBm}(k)\right\}/10\right]} \quad (mW) \qquad (13)$$

where $p_{dBm}(k)$ is the output transmission power in dBm attainable from [], $S$ is the total number of samples and $k$ is the index of these samples.

### B. Simulation Results

Fig. 7 illustrates some results where at time index 100 power controller switching occurs between two base stations. In this instance there is a difference of 20 dBm in RSSI, between the signal received at the "on-line" base station and the RSSI signal observed at the "off-line" base station. As mentioned earlier this dissimilarity in observed RSSI is due to the propagation environment and is a realistic value based on experimental observations in an indoor environment. As a result of this feedback discrepancy the system without AWBT exhibits an extremely large transient response and indeed never achieves steady state prior to completion of the simulation. The system with AWBT in place shows improvement, however there is significant time spent below $RSSI_{th}$ and as a result outage probability is still at an unacceptable level. When the modified AWBT scheme is added the outage probability is dramatically reduced highlighting the improved performance afforded by the new scheme. The results in terms of the performance criteria are summarized in table 1.

## VIII. CONCLUSION

A novel Anti-Windup Bumpless Transfer (AWBT) scheme has been presented that enables smooth, power aware switching for networked wireless healthcare applications. The new technique facilitates the continual availability of biometric information in mesh networks that arise quite naturally in an ambulatory setting. Feedback discrepancies, hardware limitations and propagation phenomena that are posed by the use of commercially available wireless communication devices were addressed using new signal processing and robust anti-windup design tools. The new AWBT scheme exhibited significant performance improvements, particularly in terms of transient behaviour at power controller switching, when compared with analogous systems operating with simple dynamic control or when only Anti-Windup (AW) methods were applied in isolation.

## ACKNOWLEDGEMENTS

The authors would like to acknowledge the support of Science Foundation Ireland under grant number 07/CE/I1147.

## REFERENCES

[1] B. Zurita Ares, C. Fischione, A. Speranzon, and K. H. Johansson. On power control for wireless sensor networks: system model, middleware component and experimental evaluation. *European Control Conference*, Kos, Greece, 2007.

[2] M. J. Walsh, S. M. Mahdi Alavi and M. J. Hayes, On the effect of communication constraints on robust performance for a practical 802.15.4 Wireless Sensor Network Benchmark problem, accepted for publication to the CDC, 2008.

[3] Yuan-Ho Chen Bore-Kuen Lee and Bor-Sen Chen, Robust Hinf Power Control for CDMA Cellular Communication Systems, *IEEE Transactions on Signal Processing*, 2006, (54)(10): 3947–3956.

[4] R. Hanus, M. Kinnaert and J. Henrotte, Conditioning technique a general anti-windup and bumpless transfer method, *Automatica*, 1987, (23): 729-39.

[5] K. Srinivasan and P. Levis, RSSI is Under Appreciated, *Third Workshop on Embedded Networked Sensors (EmNets)*, 2006

[6] IEEE Standard, Wireless lan medium access control (mac) and physical layer (phy) specifications for low-rate wireless personal area networks (lr-wpans), IEEE Std 802.15.4 (2006).

[7] M. Turner, G. Herrmann and I. Postlethwaite, Incorporating robustness requirements into anti-windup design, *IEEE Transactions on Automatic Control*, 2007, (52)(10): 1842-1855.

[8] D.S. Bernstein and A.N. Michel, A chronological bibliography on saturating actuators, *International Journal of Robust and Nonlinear Control*, 1995, (5): 375-380.

[9] P.F. Weston and I. Postlewaite, Analysis and design of linear conditioning schemes for systems containing saturating actuators, *Proc. IFAC Nonlinear Control System Design Symp*, 1998.

[10] G. Herrmann, M. Turner and I. Postlethwaite, Discrete-time and sampled-data anti-windup synthesis: stability and performance, *International Journal of Systems Science*, 2006, (37)(2): 91-114.

[11] I. Horowitz, Survey of quantitative feedback theory (QFT), *Int. J. Robust Nonlinear Control*, Vol. 11, 2001, pp. 887–921.